



# Room design for high-performance electron microscopy

David A. Muller<sup>a,b,\*</sup>, Earl Kirkland<sup>a</sup>, Malcolm G. Thomas<sup>b</sup>, John L. Grazul<sup>b</sup>, Lena Fitting<sup>a</sup>,  
Matthew Weyland<sup>a</sup>

<sup>a</sup>*School of Applied and Engineering Physics, Cornell University, Ithaca, NY 14853, USA*

<sup>b</sup>*Cornell Center for Materials Research, Cornell University, Ithaca, NY 14853, USA*

Received 19 August 2005; received in revised form 1 November 2005; accepted 5 April 2006

## Abstract

Aberration correctors correct aberrations, not instabilities. Rather, as spatial resolution improves, a microscope's sensitivity to room environment becomes more noticeable, not less. Room design is now an essential part of the microscope installation process. Previously ignorable annoyances like computer fans, desk lamps and that chiller in the service corridor now may become the limiting factors in the microscopes performance. We discuss methods to quantitatively characterize the instrument's response to magnetic, mechanical, acoustical and thermal disturbances and thus predict the limits that the environment places on imaging and spectroscopy.

© 2006 Published by Elsevier B.V.

*Keywords:* ■; ■; ■

## 1. Introduction

As electron microscopes have grown in size and sensitivity so have the requirements for the laboratories that house them. While there is considerable expertise and knowledge in the construction industry in building quiet rooms and many of the newer microscope facilities have taken advantage of this knowledge [1–5], the precise impact of the inevitable residual noise sources is less clearly understood (although there are some exceptions like AC fields and air pressure [6]). In general, one builds the best room one can for the money available, and then hopes. Costs range from \$10,000 for simple room refits to millions of dollars for new national facilities and people have generally been willing to document best practices and lessons learned [2,3,6,7]. The basic shape of a side-entry transmission electron microscope is still very similar to the designs of the early 1970s and much of the characterization of the mechanical and electromagnetic response dates back to that era [5]. Manufacturers had to re-evaluate their environmental specifications with the introduction of field

emission sources in the 1980s but until very recently based their performance specifications on recording a single transmission electron microscope (TEM) image and not scanning transmission electron microscopy (STEM) operation or TEM operations requiring multiple, correlated images or longer acquisition times. STEM images, tomographic series, energy filtering, spectroscopy and exit wave reconstructions take longer to acquire than conventional TEM images and are consequently more sensitive to very low-frequency noise sources. Issues like air pressure changes from doors opening in air-conditioned buildings become very noticeable in STEM [6] and energy loss spectroscopy can be affected by something as simple as the operator not being able to sit still on a wheeled chair.

We have previously discussed strategies for locating and reducing sources of electromagnetic interference (EMI), including common wiring mistakes that produce ground currents [6]. Vibration isolation has been extensively documented [5,8] and designs range from slab-on-grade [1,3] to suspended structures [4]. For most room environment problems, however, the key issue is location. It is very difficult to build a quiet room next to a main road, machine shop or MBE laboratory with cryo-pumps. On the other hand, if the microscope is to be located in a new building as far from the street and heavy equipment as possible, very

\*Corresponding author. School of Applied and Engineering Physics, Cornell University, Ithaca, NY 14853, USA.

*E-mail address:* [dm24@cornell.edu](mailto:dm24@cornell.edu) (D.A. Muller).

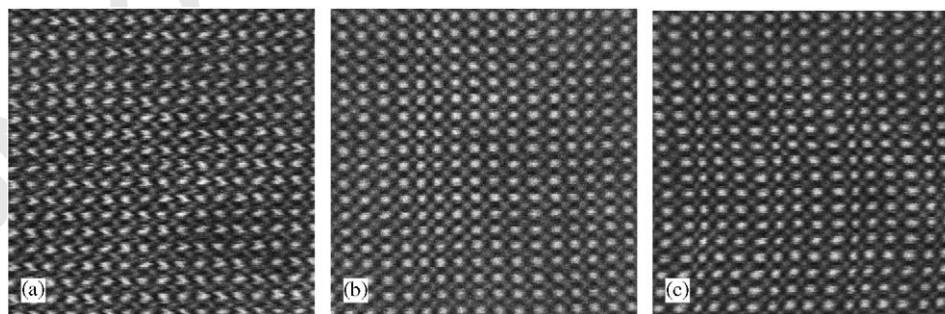
1 modest designs can yield very high performances. For  
 2 instance, we found the slab-on-grade construction for our  
 3 new microscope suite to produce floor vibrations so low (a  
 4 factor of 3 and more below the ultra-sensitive NIST-A/A-1  
 5 standards [8,9]), the microscope manufacturer's survey  
 6 team initially thought their accelerometer was broken. The  
 7 slab itself was not especially effective in attenuating  
 8 vibrations, but rather there was little in the neighborhood  
 9 to produce vibrations.

10 Air handling systems seem to be one area in which  
 11 designers are the weakest. In clean rooms, very precise air  
 12 temperature control is achieved by having rapid airflow  
 13 through the space. Needless to say, this strategy is  
 14 unsuitable for electron microscopy. Unfortunately, most  
 15 companies that build scientific laboratories seem to want  
 16 to take this high-flow approach or variations involving  
 17 extremely elaborate hollow ceilings, diffusers or circuits  
 18 to switch off the air-conditioning when taking images. A  
 19 simpler approach is to reduce the airflow and add thermal  
 20 mass to the room with radiant cooling [6,10]. This is the  
 21 approach we discuss here, as it can often be a relatively  
 22 cheap retrofit to an existing room.

23 As most environmental noise sources cannot be elimi-  
 24 nated but only reduced, it is worth establishing how  
 25 sensitive an instrument is, and how much shielding is  
 26 necessary. Or to put it another way, what happens if you  
 27 do not meet the manufacturer's room specifications? We  
 28 hope this paper will prove useful in explaining to architects  
 29 and administrators the importance and consequences of  
 30 environmental considerations.

## 31 2. The impact of AC magnetic fields on stem imaging

32 Alternating-current EMI is one of the usual suspects  
 33 whenever scan noise is observed in a STEM image. Fig. 1  
 34 shows the most common symptoms of a small AC noise on  
 35 the scan coils of a STEM. One of the first challenges is  
 36 determining when the observed noise is from EMI or  
 37 coupled through vibrations or acoustics.



38 Fig. 1. The effect of a modest AC field on an ADF-STEM image of SrTiO<sub>3</sub> recorded on a JEOL 2010F. (a) The image is recorded without any  
 39 synchronization to the external field, leading to a random tearing of the atoms. (b) External synchronization is enabled so that each scan line begins at the  
 40 same point in the AC cycle. The result is a periodic contraction and expansion of the lattice. (c) External synchronization is enabled, but the mains  
 41 frequency of the synchronization signal (AC to the scope through a UPS at ~59.9 Hz) is slightly different from the frequency of the AC noise, in this case  
 42 the building mains at 60 Hz. The result is a beating at the difference of the 2 frequencies leading to an apparent bending of the lattice, in addition to the  
 43 periodic distortions. All three conditions lead to a loss of spatial resolution in EELS where the acquisition time is longer than the mains period. The only  
 44 solution is to locate and reduce the external field.

45 The microscope column should effectively shield radio  
 46 frequency noise from the electron beam, but lower  
 47 frequencies (1–3000 Hz) are less effectively screened. To  
 48 separate EMI from other noise sources, we deliberately  
 49 applied a much larger EMI disturbance than all other noise  
 50 sources so it could be distinguished and quantified. We  
 51 have measured the field sensitivity for both our VG-  
 52 HB501A UHV-STEM and our Tecnai T20 with mono-  
 53 chromator. The procedure described below is for the  
 54 Tecnai, but is similar to the VG measurements.

55 A large (~1 m diameter) AC coil was built and placed  
 56 ~1 m from the microscope column at the same height as  
 57 the upper half of the column. The field was measured at the  
 58 column near the first condenser lens. Field variations at the  
 59 sample and gun could be 30% less.

60 Images were recorded with the external AC field on  
 61 (34 mG peak to peak), and off (0.2 mG p-p). The STEM  
 62 image scan rate was externally synchronized. Fig. 2a shows  
 63 the test sample used for the measurements before the  
 64 external AC field was applied. The structure is 5 unit cells  
 65 of SrTiO<sub>3</sub> (1.96 nm thick) grown on silicon. This marker  
 66 layer is a useful calibration standard even when atomic  
 67 resolution is lost due to the external field. Fig. 2b shows  
 68 that when the external field is applied, the synchronization  
 69 to the external field simply bends the image and the marker  
 70 layer. Knowing the width of the marker layer, we can  
 71 measure the peak-to-peak distortion in the presence of the  
 72 field.

73 At spot size 9, we found that the response was 0.52 Å/  
 74 mG (peak-to-peak), and at spot size 11, we found that the  
 75 response was 0.48 Å/mG (peak-to-peak). These are typical  
 76 STEM imaging conditions and 0.5 Å/mG can be taken as a  
 77 typical sensitivity factor. In private communications, FEI  
 78 reported a similar sensitivity for the unmonochromated  
 79 instrument and our previous experience with the JEOL  
 80 2010F suggests a similar order of magnitude sensitivity.  
 81 The VG sensitivity factor was 1.42 Å/mG. Note that many  
 82 handheld meters record the r.m.s. field, not peak-peak  
 83 value, in which case the calculated image distortion is also

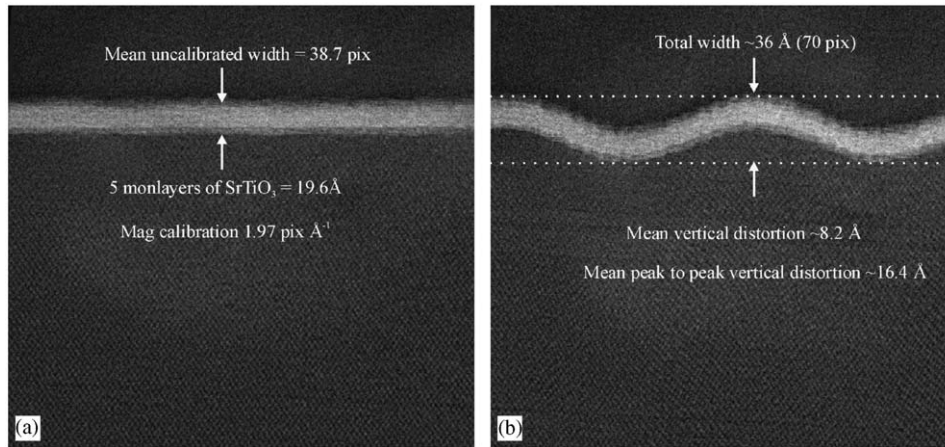


Fig. 2. Calibration of the AC-field sensitivity by applying a large external AC field to a known sample. (a) The test sample of 5 unit cells of SrTiO<sub>3</sub> (1.96 nm thick) grown on a silicon substrate imaged in a 200 kV, monochromated Tecnai F20 before the external field is applied. (b) The same sample imaged with a 34 mG peak to peak external field applied. The image is synchronized to the same scan frequency as the field. These are 512 × 512 images recorded at nominally 64 μs/pixel dwell time.

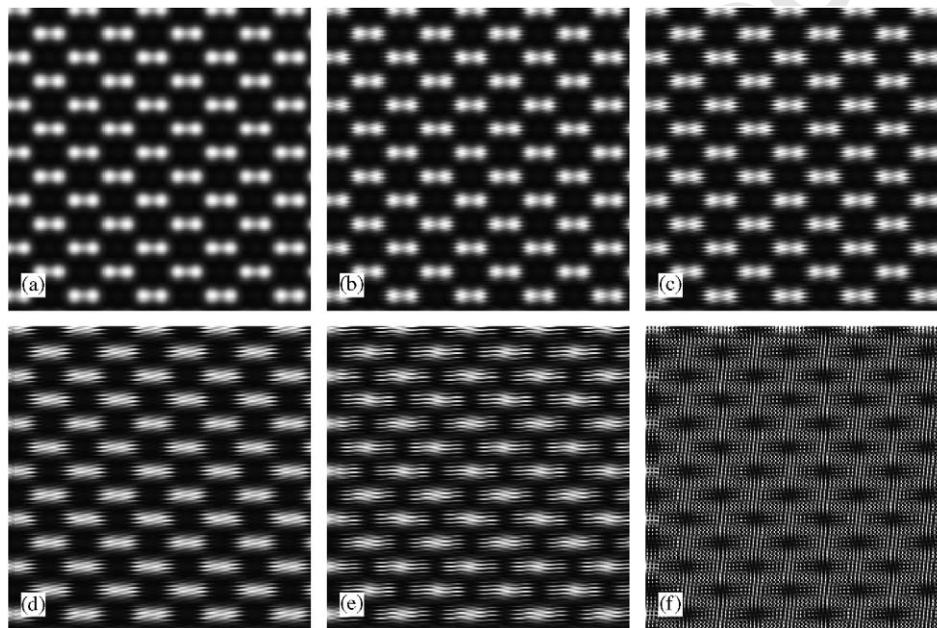


Fig. 3. Simulation of the effect of AC noise on the  $x$ -scan for Annular dark field STEM images of [1 1 0] Silicon using the field sensitivities determined from Fig. 2. (a) no noise, (b) 0.2 Å p-p (0.15 mG r.m.s.), (c) 0.4 Å p-p (0.3 mG r.m.s.), (d) 1 Å p-p (0.7 mG r.m.s.), (e) 2 Å p-p (1.4 mG r.m.s.), (f) 2 Å p-p in both the  $x$  and  $y$  scan directions. The imaging conditions are assumed to be 200 kV,  $C_s = 0.5$  mm, 10.5 mrad objective and 50 mrad ADF inner angle at optimal defocus.

an r.m.s. result. To convert from r.m.s. to p-p, multiply by ~3 for sine waves.

The standard test image favored by manufacturers in demonstrating ADF-STEM performance is most often the silicon [1 1 0] projection. Fig. 3 shows simulated ADF-STEM images for different levels of EMI interference assuming a 0.5 A/mG sensitivity factor. This figure should be useful both in understanding the visual impact of EMI on STEM imaging and also when EMI can be ruled out as a noise source. With external sync off, we would expect “image tearing” of no more than 0.1 Å p-p under normal operation conditions of our microscope (0.2 mG p-p or

0.07 mG r.m.s.). Any image distortions larger than this (and originally we did have some) cannot be blamed on EMI, and their source must lie elsewhere. In our case, this led us to uncover and fix some scan electronics and acoustic noise problems.

It is not only the scan system that is sensitive to AC fields. Post-column spectrometers show a typical sensitivity of about 1 eV/mG. EMI can reduce the energy resolution, especially for monochromated systems. Quasi-DC fields from elevators, metal in movable furniture or passing traffic can shift the energy alignment during EELS mapping, making it very difficult to extract reliable core-

1 level shifts. Only somewhat tongue-in-cheek we had  
 2 previously calibrated the response to external traffic in  
 3 terms of engine size [6], but for heavy vehicles, it turns out  
 4 an easier estimate follows from the advice of our local fire  
 5 department that truck axles typically are designed to  
 6 support about 20,000 lbs per axle so the weight of the truck  
 7 can be guessed simply by counting axles. Most of this  
 8 weight is magnetic and so from measurements of fire  
 9 engines driven past our field meter, we find that the  
 10 magnetic field produced is  $B_{\text{truck}} \sim 0.1 \text{ mG/axle}$  at 25 ft and  
 11 falls off between  $1/\text{distance}^2$  and  $1/\text{distance}^3$  depending on  
 12 ~~the~~ whether the truck is near or far.

### 13 3. Magnetic field remediation

14 When it is not practical to eliminate the source of EMI,  
 15 there are a number of different strategies to screen out the  
 16 fields at the column. The oldest and most expensive  
 17 approach is to construct a shielded room made from a  
 18 high permeability material such as mumetal. Slowly  
 19 varying magnetic fields are not strongly attenuated.  
 20 Instead, magnetic shielding works by providing a low  
 21 reluctance path for external fields. Consequently, it is only  
 22 effective if it closes the instrument on all sides. Placing  
 23 shielding on only 1 wall is not very effective. As a rough  
 24 rule of thumb, the magnetic field will penetrate roughly 5  
 25 times the size of any hole in the shielding. The shielded  
 26 room also needs to be quite large, as any fields inside the  
 27 room will also induce image fields in the walls. Further, the  
 28 walls of a mu-metal shield room need to be very rigid  
 29 otherwise it is possible to couple acoustic and mechanical  
 30 vibrations into magnetic fields of the same frequency. The  
 31 amount of space required to house and service a TEM/  
 32 STEM makes such rooms rather expensive. Simply  
 33 choosing a large room (with a high ceiling) for the  
 34 microscope may be as effective since most fields decay  
 35 rapidly with distance.

36 Another approach to shielding is eddy current shielding  
 37 with a good conductor. Here the fields are attenuated so  
 38 the shield need not be continuous. Typical costs range from  
 39 \$10,000–40,000. The thickness of shielding material re-  
 40 quired is determined by its skin depth (in meters) of

$$41 \delta = \sqrt{\frac{2}{\sigma\mu\omega}}, \quad (1)$$

42 where  $\sigma$  is the conductivity,  $\mu$  is the magnetic permeability  
 43 of the material, and  $\omega$  is the frequency of the incident  
 44 radiation [11]. An electromagnetic wave incident upon a  
 45 highly conducting medium is exponentially attenuated over  
 46 a skin depth. Popular shielding materials are good  
 47 conductors like aluminum (copper is usually too expensive)  
 48 or high-permeability, low-loss conductors like transformer  
 49 core steel. The skin depth of Al is  $\sim 5 \text{ mm}$  at 60 Hz so a 1 cm  
 50 thick Al liner will attenuate external fields by a factor of  $\sim 7$   
 51 and 2 cm thick by  $\times 50$ . The cost effectiveness of  
 52 conventional and high-conductivity Al alloys can be

53 evaluated by noting that the skin depth scales as the  
 54 square root of resistivity. If only low attenuation factors  
 55 are required there is not much difference, but small  
 56 differences in exponentials add up and for high attenua-  
 57 tions the required thicknesses are noticeably different. The  
 58  $1/\sqrt{\omega}$  dependence of the skin depth makes this screening  
 59 most effective at higher frequencies, and almost completely  
 60 useless for quasi-DC disturbances (like elevators or nearby  
 61 trains).

62 An effective companion method to eddy current shield-  
 63 ing is active field cancelation with a wideband (including  
 64 DC) sensor. AC sensors are more sensitive at higher  
 65 frequencies, but these should already have been screened  
 66 out by the eddy current shielding. Active cancelation works  
 67 best for compensating fields from distant sources (which  
 68 hopefully elevators and trains are). In the simplest versions,  
 69 loops of wire are run around the room to produce  
 70 Helmholtz coils in the  $x$ ,  $y$  and  $z$  directions. These can  
 71 exactly cancel out a field at one point in the room so the  
 72 location of the feedback sensor is important. For a small  
 73 room, canceling the field at the gun would have the effect  
 74 of enhancing the field at the spectrometer. For the same  
 75 reasons, these active-cancelation systems are not always  
 76 effective in compensating for nearby or non-uniform  
 77 sources of fields such as improperly grounded conduits or  
 78 wiring in the room. More sophisticated versions of the  
 79 cancelation system can have multiple meshes of coils to  
 80 provide a more uniform response. In dealing with DC  
 81 fields, long-term sensor drift has to be very small or else a  
 82 steady image and alignment drift will be observed on the  
 83 microscope. As a stand-alone system, active field cancela-  
 84 tion should not be expected to eliminate all random noise  
 85 as the microscope column is often more sensitive to low-  
 86 frequency stray fields than the AC sensor of the cancelation  
 87 unit. For well-defined frequencies (e.g. mains), a factor of  
 88 20–30 might be typical, but reducing low frequencies and  
 89 residuals below 1 mG can be difficult.

### 90 4. Characterizing mechanical and acoustic noise sources

91 Quoting a single number for the sensitivity of a  
 92 microscope to mechanical or acoustic noise is often not  
 93 practical. The noises are less likely than EMI to be at one  
 94 set frequency and each microscope's resonances where it is  
 95 particularly sensitive to noise will differ from instrument to  
 96 instrument. Some general trends are that tall, thin columns  
 97 will be more likely to sway in the breeze (yes, air movement  
 98 will do that) than short fat ones; the vibration isolation on  
 99 most microscopes do a pretty good job of damping out  
 100 vibrations above 100 Hz or so but can amplify noise at  
 101 1–10 Hz depending on their resonance frequency. This can  
 102 be a problem as many buildings can also have their natural  
 103 frequencies around 5–10 Hz. If the vibration frequency is  
 104 above a few hundred hertz, it is more likely to be coupled  
 105 acoustically via the sample holder.

106 Fig. 4 illustrates this point. Fig. 4a shows the vibration  
 107 spectrum measured with a Wilcox accelerometer (Spicer  
 108

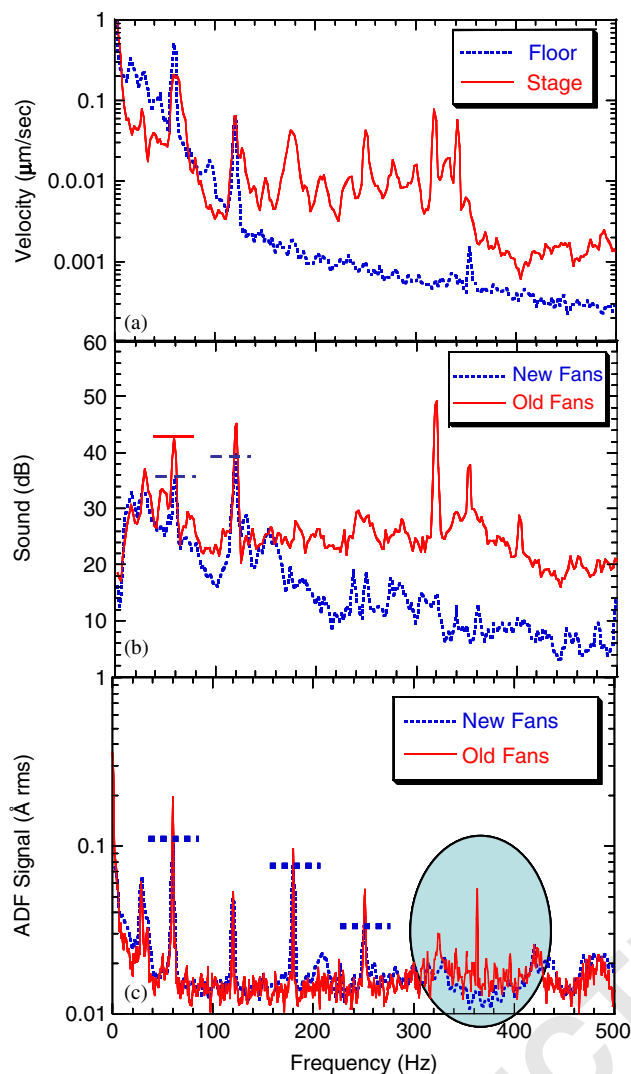


Fig. 4. Troubleshooting noise sources from their spectral fingerprints. (a) Mechanical vibration spectra for an accelerometer placed on the floor and the column of the microscope showing the noise from 200–400 Hz is not coming through the floor. (b) A sound meter shows that the computer fans produce a noticeable noise component in this frequency range. (c) A spectrum analyzer connected to the ADF photomultiplier preamp output, as described in the text, shows the reduction in scan noise when the computer fans were replaced with quieter ones.

Instruments) both on the floor of the room below the microscope column, and on the microscope column at the goniometer. Below 60 Hz, there is more noise on the floor than the column; however, above 60 Hz, the stage is shaking more than the floor. There are also sharp resonances between 300 and 400 Hz that are different for the floor and stage. This suggests that the mechanical isolation of the microscope is working correctly—and in this case is protecting the floor from being shaken by the column!

The sharp resonances provide an easy fingerprint to isolate the noise source. Fig. 4b shows the acoustic spectrum in the room—most of the noise is from the fan in computer controlling the microscope. The fans in the Gatan camera controller were off for this experiment as

they are even louder. As the column has a large surface area (and thanks to the vibration isolation is free to rock), it will move a few microns in response to sounds or air movements—basically any air pressure wave.

To assess the impact of these acoustic disturbances we set the microscope up in ADF-STEM mode and stopped the beam on the midpoint of an edge of a gold particle. (Placing the beam on the side of an atom column if an atomic resolution image can be formed works as well—this was used to obtain the spectra in Fig. 4.) If there is no noise pickup in the microscope or its scanning system, the beam should remain stationary and the ADF photomultiplier signal should be constant. Any slow drift can be corrected from observing the Ronchigram. However, any noise source will shake the beam, causing the signal to rise and fall as the beam moves on and off the edge of the particle. By feeding the ADF signal into a signal-averaging spectrum analyzer, a complete noise spectrum can be built up. Typically, a hundred or so spectra need to be averaged together to give a clear picture of the noise. Detector noise can be distinguished by defocusing the beam so it is no longer sensitive to changes in position. This signal is only proportional to the beam deflection. For an absolute calibration, we use the results of the previous section to scale the noise peak at 180 Hz, which is almost solely due to EMI interference. Fig. 4c shows the noise in the ADF signal before and after we replaced the fans on the computer with low-noise PC fans. The old fans excited a mechanical resonance in the microscope around 350 Hz. The new fans do not, and generally reduce the other harmonics as well.

## 5. Acoustic remediation

Fig. 4b shows that the microscope was also sensitive to acoustic noise at 60 Hz and below. Acoustic shielding at these low frequencies is difficult. Conventional sound damping material made from polyurethane or other foams are almost completely ineffective in the 0–125 Hz band. To get some feeling for the length scales involved, consider that a 30 Hz sound wave will have a wavelength of about 10 m, about the size of a larger microscope room. Rather than thinking of sound waves bouncing off walls and following well-defined geometric rays, it is more useful to think of the room as a resonant cavity. The fixed walls of the room force the air velocity to zero and the pressure fluctuations to a maximum at the walls. The pressure fluctuations will drive volume changes in objects in the room (like the microscope). However, these volume changes are adiabatic at audio frequencies and intensities—i.e. heat cannot be transferred out of the wave by compression and expansion of the air [12]. Another mechanism is needed for attenuation. For porous materials such as fiberglass, the sound wave's kinetic energy is converted to frictional heat as fibers are set in motion (see chapter 9 of Ref. [13] for a more detailed discussion). Since the sound wave's kinetic energy is proportional to the

1 square instantaneous local air velocity, most of the sound's  
 3 kinetic energy is peaked somewhere in the middle of the  
 5 room—where the microscope is. Placing acoustic damping  
 7 materials on the wall also places it at velocity nodes (and  
 9 hence kinetic energy minima) of the sound wave, where it is  
 11 least effective in absorbing acoustic energy. The recom-  
 13 mended practice for low-frequency sound absorption is to  
 15 leave a gap between the damping material and the wall [14].  
 17 Even leaving a 6 in. gap between the sound damp and the  
 19 wall has a noticeable effect.

11 Since the wavelength of low-frequency sounds is so much  
 13 larger than any damping material, the shape and pattern of  
 15 damping material is not too critical. Fiberglass proves to be  
 17 very efficient in absorbing these sounds. Fiberglass acoustic  
 19 banners are often used to deaden noise in large spaces like  
 21 gymnasiums and factories. Consequently, they tend to be  
 23 much cheaper than the eggshell foams used to damp high  
 25 frequencies in recording studios or the panels used in office  
 27 space. We used Alphaflex 4" ripstop nylon banners (10 × 4)  
 29 acoustic banners from Acoustical Solutions ([www.acoustical-solutions.com](http://www.acoustical-solutions.com)) and hung them 6 in. off the walls and in  
 31 the middle of the room off the ceiling (Fig. 5). The banners  
 33 do a good job at low frequencies, damping noise from  
 35 motors, chillers and AC equipment (<100 Hz), but there  
 37 are better materials if higher frequencies (such as from  
 39 computer fans) are the problem.

27 A very rough rule of thumb is that side entry stages will  
 29 pick up about 0.1 Å at 40 dBC and 0.3 Å at 50 dBC noise  
 31 level, although this will vary considerably depending on the  
 33 noise source. Or put another way, if you can hear it, and it  
 35 sounds loud, the microscope probably feels the same way.  
 37 In the quasi-static limit, pressure changes from doors  
 39 opening in air-conditioned buildings or storm fronts  
 41 approaching can cause drifts of 1 Å/Pa [6].



55 Fig. 5. Photograph of the STEM room at Bell Labs circa 2002. Fiberglass acoustic banners are hung ~6 in off the wall and behind the radiant cooling  
 57 panels. When filled with water, the cooling panels are rather poor sound reflectors. The air supply to the room is connected to a duct sock which diffuses  
 air along its entire length, rather than in drafts as with vented supplies.

## 6. Temperature control

Poor temperature control does not add scan noise but rather produces long-term drifts to imaging and spectroscopy. However, drafts from air inlets can cause serious distortions to STEM images. These tend to be turbulent and not at a single frequency so are hard to spot from a spectrum analyzer. In STEM images, their effects are most noticeable at low frequencies (10 Hz and below), producing random deflections—especially line to line. The microscope's vibration isolation usually has a resonance frequency of a few hertz so it is especially sensitive to air movements. Consider a room where the AC system is producing 50 dB of noise—a fairly quiet room. This corresponds to a pressure of 6 mPa. The microscope has a cross-sectional area of about 1 m<sup>2</sup> so the force on the column is 6 mN. We can use Hooke's law ( $F = -kx$ ) to estimate the displacement of the column: with a resonance frequency of 5 Hz and a mass of ~1000 kg, the spring constant of a microscope is  $k = m\omega^2 \approx 10^6$  N/m. The quasi-static displacement of the column is then  $x \sim 6 \times 10^{-9}$  m or 6 nm. The actual impact is fortunately attenuated when the stage can move in phase with the column; nevertheless, this argument does demonstrate the vulnerability of a seemingly immovable object to a tiny breeze. (We checked this with an accelerometer and the column itself does indeed move detectably when people talk or blow on it.) Airflow at the column should not exceed 30 ft/min and ideally be less than 15 ft/min. This can be checked with the "toilet-paper test" [6]: take a single-ply strip of toilet paper, cut it into 1 ft long and  $\frac{1}{8}$  in. wide sections. Decorate the room. If the strips deflect by more than an inch at the bottom, the airflow exceeds 20 ft/min.

The first priority in designing an air handling system should be to minimize air movement in the room. Forced air systems remove all heat from the room by convection and conduction. However, the heat capacity of air is very low, and requires large airflows to remove large heat loads (see Ref. [6] for airflow calculations). Whenever possible, as much of the heat-generating equipment such as power distribution racks should be kept out of the room. Next, the air into the room should be diffused as much as possible. A false ceiling with multiple perforations works, but is expensive to retrofit. A more effective and cheaper solution is to add a duct sock to the air inlet. This is essentially a nylon stocking where the air diffuses out uniformly along the length of the sock through weave in the fabric. These socks also reduce the airflow into the room and must be sealed tightly to the inlet or air can escape with a loud whistling sound. We have used duct socks from [www.ductsox.com](http://www.ductsox.com) (usually 20–30 ft of the Stat-X low-thru model). This is an easy retrofit and often cheaper than sheetmetal ductwork in the first place.

The less heat that has to be removed by air movement, the more stable the room. We have found that radiant cooling is an effective (and often the cheapest) method of controlling the room temperature or at least add thermal mass to the room. This can be as simple as a large surface-area radiator on the wall with building chilled water flowing through it. If this removes most of the heat load, then the existing forced-air system can be slowed down, and used mostly to regulate humidity (which radiant cooling cannot). More sophisticated systems are described by Roulet et al. [10]. These can regulate the temperature to better than  $0.1^\circ\text{C}$ , and as most of the cooling is by radiation, the return to equilibrium is rapid. Fig. 5 shows the radiant cooling panels, from Energy Solaire, that we have used in our microscope room designs (both Bell Labs in 2002 and Cornell in 2004). A typical system will use 10–20 cooling panels (each with an area of  $2\text{ m}^2$ ) fed by an old microscope chiller. Fig. 6 shows the effect on room temperature stability, with and without a radiant cooling system added to our microscope room at Cornell. The key was tuning the water temperature into the range that the building AC system was no longer switching on the heating or cooling coils. We have to adjust the water temperature once in spring, and again in the fall. We are currently designing a controller to provide active feedback from the room temperature instead of the water temperature to the system. Even without room temperature feedback, the stability over a week can be  $0.1^\circ\text{F}$  or better.

The benefits of the radiant cooling system are reduced drift for both imaging and spectroscopy as the spectrometer and high-tension supply are sensitive to temperature changes. Fig. 7 shows one additional benefit of a stable room: frame averaging. Instabilities—especially air and pressure changes—cause local bend and distortions in STEM lattice images. Once these instabilities are reduced below about a fifth to a tenth of lattice spacing, correlating and adding successively recorded images becomes a

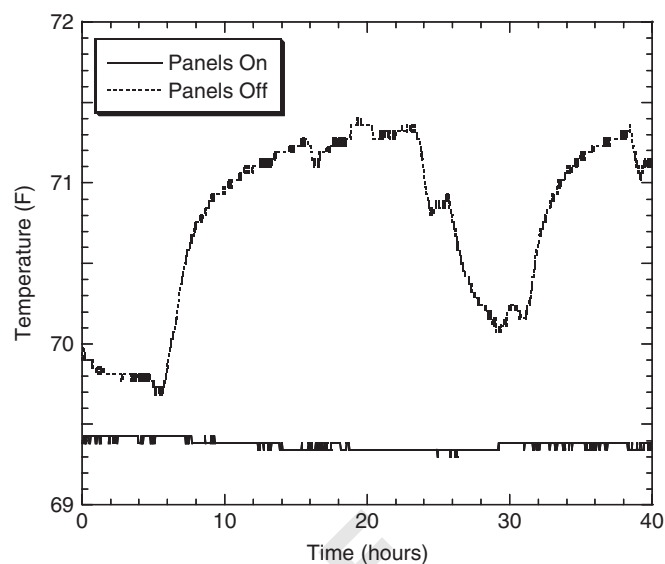


Fig. 6. Room temperature recorded in the STEM room (a) with the radiant cooling panels off and (b) the panels on and water temperature adjusted so that the building AC system hot and cold water valves are closed.

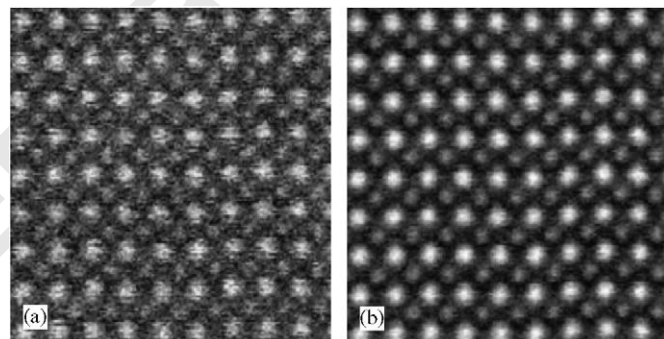


Fig. 7. High-Angle annular dark field lattice images of  $\text{SrTiO}_3$  recorded on our monochromated Techni-T 200 kV with a 40 mrad collection angle, and 9.6 mrad incident angle. The bright atoms are Sr, and the fainter ones are Ti. (a) at  $32\ \mu\text{s}/\text{pixel}$ , (b) The average of 10 cross-correlated images, each recorded at  $32\ \mu\text{s}/\text{pixel}$ . Both images are  $33\ \text{\AA}$  full scale.

practical method to increase signal to noise and average out the remaining scan noises. As frame averaging trades off resolution for signal, it is only practical in a quiet environment.

## 7. Summary

We have described some common sources of environmental noise and presented strategies to identify and remediate these problems in a cost-effective manner. For instance, how low should the external magnetic fields in the room be made? A serious consideration when a shielded room could cost up to \$300,000. For most microscopes, we have measured the beam deflection to be  $0.5\ \text{\AA}/\text{mG}$  of AC field at 60 Hz. Typically, such instruments produce roughly  $0.1\ \text{mG p-p}$  ( $0.03\ \text{mG r.m.s.}$ ) of AC noise from their own

1 internal electronics and pumps, suggesting that until  
 2 substantial redesigns are made, 0.1–0.2 mG p-p is a  
 3 reasonable limit for external AC fields.

4 For post-column EELS spectrometers, the sensitivity is  
 5 around 1 eV/mG, suggesting that 0.1 eV stability is achiev-  
 6 able in a quiet room. Microscope rooms should be at least  
 7 50 ft from roads, loading docks, elevators and other  
 8 sources of quasi-DC magnetic fields. We found that side-  
 9 entry stages are sensitive to air pressure changes and  
 10 acoustic pickup, especially at stage resonances. Roughly  
 11 0.1 Å distortions result from 40 dBC noise levels and 0.3 Å  
 12 at 50 dBC. Air pressure changes can cause image deflec-  
 13 tions as large as 1 Å/Pa, but this does depend on the stage  
 14 design.

#### 15 Acknowledgments

16 Support for this work was provided by the Cornell  
 17 Center for Materials Research, an NSF MRSEC, and NSF  
 18 Grant # DMR-0417392 for the acquisition of the high-  
 19 resolution spectrometer. Helpful discussions with Moham-  
 20 mad Daraei of FEI on column and stage resonances are  
 21 acknowledged.  
 22  
 23

#### References

- 25
- [1] E. Ungar, D.H. Sturz, H. Amick, *Sound Vib.* 24 (1990) 20. 27
- [2] J.H. Turner, M.A. O'Keefe, R. Mueller, in: G. Bailey (Ed.),  
*Proceedings on Microscopy and Microanalysis*, vol. 3, San Francisco  
 Press, 1997, p. 1177. 29
- [3] M.A. O'Keefe, et al., *Microsc. Today* 12 (2004) 8. 31
- [4] C.E. Brown, et al., *Microsc. Today* 12 (2004) 16. 31
- [5] R. Anderson, in: A.M. Glauert, (Ed.), *Practical Methods in Electron  
 Microscopy*, vol. 4, North-Holland, Amsterdam, 1975, p. 1. 33
- [6] D.A. Muller, J. Grazul, *J. Electron Microsc.* 50 (2001) 219. 33
- [7] C.J.D. Hetherington, et al., in: *Materials Research Society Symposi-  
 um Proceedings*, vol. 523, MRS, 1998, p. 171. 35
- [8] H. Amick, *J. Inst. Environ. Sci.* 40 (1997) 35. 37
- [9] H. Amick, et al., in: *Proceedings of SPIE: Buildings for Nanoscale  
 Research and Beyond*, vol. 5933, SPIE, San Diego, 2005, p. 1. 37
- [10] Y. Roulet, et al., *Energy Buildings* 30 (1999) 121. 39
- [11] D.H. Staelin, A.W. Morgenthaler, J.A. Kong, *Electromagnetic  
 Waves*, Prentice-Hall, Englewood Cliffs, NJ, 1998. 39
- [12] M.W. Zemansky, R.H. Dittman, *Heat and Thermodynamics*, sixth  
 ed., McGraw-Hill, New York, 1987. 41
- [13] F.A. Everest, *Master Handbook of Acoustics*, fourth ed., McGraw-  
 Hill, New York, 2001. 43
- [14] *Noise Control: A Guide for Workers and Employers*, Occupational  
 Safety and Health Administration, US Department of Labor,  
 Washington, DC, 1995, p. 63. 45

UNCORRECTED PROOF